



## Grain refinement of gravity die cast secondary AlSi7Cu3Mg alloys for automotive cylinder heads

Giordano CAMICIA, Giulio TIMELLI

Department of Management and Engineering, University of Padova, Stradella S. Nicola, 3 I-36100 Vicenza, Italy

Received 22 July 2015; accepted 7 January 2016

**Abstract:** The effects of AlTi5B1 grain refinement and cooling rate on the microstructure and mechanical properties of a secondary AlSi7Cu3Mg alloy were reported. Metallographic and image analysis techniques have been used to quantitatively examine the macrostructural and microstructural changes occurring with the addition of grain-refining agent at different cooling rates by using a step casting die. The results indicate that the addition of AlTi5B1 produces a fine and uniform grain structure throughout the casting and this effect is more pronounced in the slowly solidified regions. Increasing the cooling rate, lower amount of grain refiner is necessary to produce a uniform grain size throughout the casting. On the other hand, the initial contents of Ti and B, present as impurity elements in the supplied secondary alloy, are not sufficient to produce an effective grain refinement. The results from the step casting geometry were applied to investigate a gasoline 16V cylinder head, which was produced by gravity semi-permanent mould technology. The grain refinement improves the plastic behaviour of the alloy and increases the reliability of the casting, as evidenced by the Weibull statistics.

**Key words:** aluminium alloy; grain refinement; step casting; cylinder head; cooling rate; microstructure; mechanical properties

### 1 Introduction

Aluminium alloys are widely used in the transport industry due to their relatively low density. They allow approximately a 50% weight saving over competing ferrous materials. Lightweighting is one of the most effective impacts on fuel consumption and CO<sub>2</sub> emissions: as 100 kg saving on the mass of a car is equivalent to a reduction of 0.35 L of fuel per 100 km and 9 g of CO<sub>2</sub> per km, respectively [1].

The cylinder head, along with cylinder block, valvetrain, crankshaft and pistons, and connecting rod assembly, is one of the main components of internal combustion engines. It conveys air and gasoline to the combustion chamber and serves as a cover for the cylinders. The cylinder head must be strong and rigid to distribute the gas forces acting on the head as uniformly as possible through the engine block [2]. In order to resist the high combustion pressure, it is demanded to develop high strength materials and innovative processes for the production of cylinder heads.

Aluminium alloys are increasingly being used to

produce cylinder heads due to the favourable ratio between mechanical strength and low density, and good thermal conductivity. In Europe, cast iron cylinder heads have been almost completely replaced by cast Al alloys during the past 20 years. This replacement is particularly evident for engines equipping light duty vehicles, like personal cars and light commercial vehicles.

Base materials used for aluminium cylinder heads are hypoeutectic primary Al–Si foundry alloys, whose final microstructure consists of a primary Al-rich phase, with an Al–Si eutectic structure made by hard and brittle plate-like eutectic Si phase in a softer Al matrix. The modification of the eutectic Si from a detrimental plate-like morphology to a fine and fibrous structure can be achieved in two different ways: by rapid cooling during the solidification [3] or by adding small amounts of modifying elements, such as Na and Sr.

Further, Mg and Cu are typically present in order to improve the fatigue performance and the high temperature resistance of the Al–Si alloys, respectively. Innovative Cu-containing alloys have been developed specifically for high performance diesel engines (e.g., AlSi7MgCu0.5, AlSi9Cu1Mg), providing strength and

hardness even without post-casting heat treatment [4,5].

Even if the selection of the alloy composition can be optimised according to the specific design and casting conditions of the component, it is however important to find a compromise between high mechanical properties and reasonable material cost. For this reason, the diffusion of secondary Al foundry alloys is increasing in the Al foundry. The secondary Al alloys show lower cost than primary ones, but present small amount of elements and impurities, with wider composition tolerance limits with respect to primary alloys. These characteristics are a consequence of the recycling process and can have negative effects on the mechanical properties and final quality of the components [6]. Therefore, in order to satisfy all the product requirements, a proper control of the as-cast microstructure by the application of preliminary processes, such as grain refinement and eutectic modification, is generally necessary [7].

Chemical grain refinement is commonly used in sand and gravity Al foundries for automotive castings to ensure fine and equiaxed grains [8–10]. The Al–Ti–B master alloys, in particular AlTi5B1, are widely used as grain refiners [11]. Several works, mainly referred to primary foundry alloys, have been carried out on grain refinement, revealing how the TiB<sub>2</sub> particles present in the Al–Ti–B master alloys are the germ for the heterogeneous nucleation [12], but they become efficient grain refiners only with an excess Ti content [13,14]. This excess can not only increase the nucleating potency of TiB<sub>2</sub> particles, but also reduce the grain growth of primary  $\alpha$ (Al) crystals during the solidification. Using Al–Ti–B master alloys, a content of 0.10%–0.15% Ti (mass fraction) is generally added to primary Al alloys [8].

On the other hand, the studies on grain refinement of secondary Al–Si alloys are limited. The application of a preliminary melt treatment for grain refinement can effectively reduce the detrimental effect of impurities, by reducing the size of the brittle phases formed by the high level of impurities [15]. However, it has also been demonstrated that the presence of these impurity elements can affect the degree of grain refinement itself [16] or decrease the efficiency of Al–Ti–B grain refiners [17,18].

In this work, the grain refinement of a gravity die cast secondary AlSi7Cu3Mg alloy for automotive cylinder heads has been studied. Firstly, the study

focused on a step casting, where different solidification conditions occurred according to the wall thickness of each step. Further, the results were used to develop the grain refining process of an automotive gasoline 16V cylinder head, which was produced by gravity semi-permanent mould technology.

## 2 Experimental

### 2.1 Casting alloys

A secondary AlSi7Cu3Mg cast alloy was supplied as commercial secondary alloy in the form of ingots and used as a base-line. The ingots were pre-heated at (150±10) °C and subsequently brought to the melting temperature at (780±10) °C. The chemical composition of the supplied base alloy (Alloy 0), measured on separately poured samples, is shown in Table 1. The molten metal was tapped from the furnace, skimmed and treated according to the standard foundry practice. The reduced pressure test was performed to evaluate the molten quality after degassing. Density values higher than 2.66 g/cm<sup>3</sup> were measured during the experimental campaign. The liquid metal was then transferred to an holding furnace where grain refinement and eutectic modification were carried out. Hydrogen content of the melt in the holding furnace was analysed by Foseco ALSPEK H<sup>®</sup> analyser, and it was almost constant at 0.20 mL/100 g Al.

Three different alloy configurations were designed in the experimental plan: base alloy (Alloy 0); base alloy + 0.01% Sr (mass fraction) (Alloy 1); base alloy + 0.01% Sr + 0.125% Ti (mass fraction) (Alloy 2).

Grain refinement and eutectic modification were achieved by properly adding weighed AlTi5B1 and AlSr3.5 rods into the molten base alloy to ensure that the Ti and Sr levels reached the desired levels. The chemical compositions of the experimental alloys are indicated in Table 1.

### 2.2 Step casting

In order to evaluate the combined effects of grain refinement and cooling rate, a step casting die was used. A detailed description of the permanent step mould design, the casting procedure, and the process parameters was given elsewhere [19,20]. Briefly, the step casting presented a range of thickness from 5 to 20 mm and it was gated from the side of the thinnest step, while the

**Table 1** Chemical compositions of experimental alloys (mass fraction, %)

Alloy No.	Si	Fe	Cu	Mn	Mg	Zn	Cr	Ni	Ti	B	Sr	Al
0	7.26	0.620	3.15	0.344	0.357	0.570	0.033	0.035	0.0411	0.0012	0.0001	Bal.
1	7.27	0.634	3.09	0.348	0.351	0.550	0.034	0.035	0.0397	0.0008	0.0114	Bal.
2	7.25	0.631	3.13	0.350	0.365	0.570	0.032	0.034	0.1270	0.0180	0.0108	Bal.

riser, over the casting, ensured a good feeding. The die cavity had a filter seat before the gating system, where a Foseco SIVEX foam filter with medium porosity was placed before each casting. The mass of the Al alloy casting, including the runner system, was about 1.8 kg.

A semi-permanent layer of boron nitride coating was sprayed on the AISI H11 die walls at temperature of about 200 °C according to standard foundry practice. Before pouring, the temperature of the die was increased up to (350±10) °C. The temperature of the die was measured by means of thermocouples embedded in the die in order to ensure a good reproducibility of the tests. The working temperature in the die was in the range of 380–450 °C.

### 2.3 Cylinder head

To analyse the effects of grain refinement on real complex-shaped castings, an automotive gasoline 16V cylinder head (Fig. 1), which was produced by gravity semi-permanent mould technology, was cast by using alloys 1 and 2 (see Table 1). The mass of the Al alloy casting was respectively 12.8 or 6 kg, including or without the runner system and the riser. The melt was automatically transferred from the holding furnace to the die by means of a coated ladle.

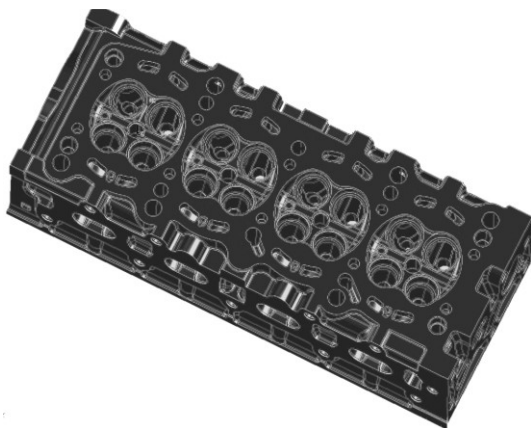


**Fig. 1** Geometry of gasoline 16V cylinder head analysed (View from the side of the flame deck showing the bowl shaped cavities, typical of gasoline cylinder heads)

### 2.4 Metallographic characterisation

Generally, cylinder heads, produced with gravity casting process, show high solidification rates in the flame deck region, resulting in a fine microstructure with low defect content and hence good mechanical properties; on the contrary, the bolt bosses present coarser microstructure due to greater wall thickness and lower cooling rate. These regions are the most thermally and mechanically stressed ones, therefore, the evaluation of microstructure is mandatory, as required by most of the customers' specifications. On the other hand, the step

casting' design allows to obtain a range of solidification rates and consequently different microstructures in one pour. Here, the 5- and 15-mm steps show cooling rates similar to those obtained in the flame deck and bolt bosses, respectively.

Therefore, the 5- and 15-mm thick steps were sectioned along their main axis at half width, while the cylinder heads were sectioned parallel to the flame deck (~4 mm under the casting surface) and transversally along the bolt bosses.

In order to evaluate the microstructure, the specimens were prepared up to 3 µm finish with diamond paste and, finally, polished with a commercial fine silica slurry for metallographic investigations. Microstructural analysis was carried out using an optical microscope and quantitatively analysed using an image analyser.

The image analysis was focused on the secondary dendrite arm spacing (SDAS), and on the size and morphology (aspect ratio) of the eutectic silicon particles. The linear intercept method was used to measure the SDAS. This method entails drawing a straight line perpendicular to the growth direction of aligned groups of secondary cells to indicate dendrite arms for measurements; the value of SDAS is then calculated as the ratio between the length of the intercept line and the number of the secondary cells. The size of eutectic Si particles is defined as the equivalent circle diameter ( $d$ ), while the aspect ratio ( $\alpha$ ) is the ratio of the maximum to the minimum Ferets. To obtain a statistical average of the distribution, more than 1000 particles from each specimen were analysed.

To quantitatively calculate the grain size, the polished specimens were etched in concentrated Keller's reagent (7.5 mL HNO<sub>3</sub>, 2.5 mL HF, 5 mL HCl and 35 mL H<sub>2</sub>O) and further in a HNO<sub>3</sub> solution to improve contrast [21]. The grain size was then measured using the Heyn linear intercept procedure, according to the ASTM standard E112-12 [22].

### 2.5 Tensile testing

Round tensile specimens were machined from the regions of the flame deck (P1–P4) and along the bolt bosses (C1–C4), as indicated in Fig. 2. The tensile specimens had a total length of 100 mm and gauge length and diameter of 25 and 5 mm, respectively.

Though the melt quality was monitored during the cylinder heads manufacturing by evaluating the density and hydrogen content as described in Section 2.1, radiographic inspections were further carried out on the tensile specimens before mechanical testing in order to assure an acceptable level of soundness and to localise the porosity distribution.

At least 20 tensile tests were done for each alloy

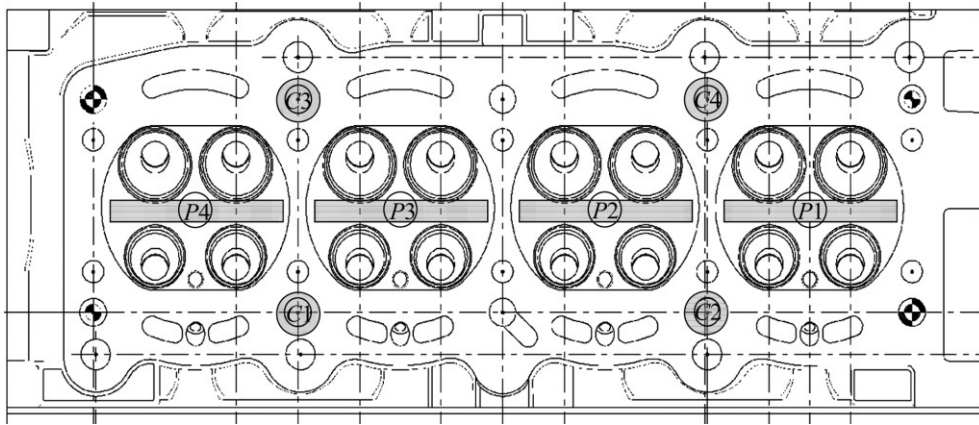


**Fig. 2** Locations of specimens for mechanical testing and metallographic investigations: Flame deck (P1–P4) and bolt bosses (C1–C4)

according to the standard ISO 6892–1:2009 [23]. The crosshead speed was 2 mm/min. The strain was measured using a 25 mm extensometer. Experimental data were collected and processed to provide yield stress (YS, actually 0.2% proof stress), ultimate tensile strength (UTS) and the elongation to fracture ( $s_f$ ) and quality index ( $Q$ ), which was developed by DROUZY et al [24]. If the flow stress–strain curve is described by the Hollomon law:

$$\sigma_t = K(\varepsilon_t)^n \quad (1)$$

The quality index takes into account the UTS ( $\sigma_b$ ) and  $s_f$  in the equation [25]

$$Q = \sigma_b + 0.4K1g s_f \quad (2)$$

where  $\sigma_t$  (MPa) and  $\varepsilon_t$  are true stress and true plastic strain, respectively;  $n$  is the strain hardening exponent and  $K$  (MPa) is the material's strength coefficient. The quality index, combining both strength and ductility, can be more descriptive of alloy tensile properties.

The two-parameter Weibull analysis was then applied to accurately describing the distribution of tensile properties of the alloys [26]. The slope of the linearised Weibull plot, known as Weibull modulus  $\beta$ , represents an index of the reliability of the experimental data. According to GREEN et al [27], this parameter seems to be more important than the average mechanical properties.

## 3 Results and discussion

### 3.1 Macrostructural observations

#### 3.1.1 Step casting

Typical macrostructures of step castings after Sr modification and grain refinement treatment are shown in Fig. 3. In the base alloy, as well as after Sr addition, the grain structure becomes coarser by increasing the

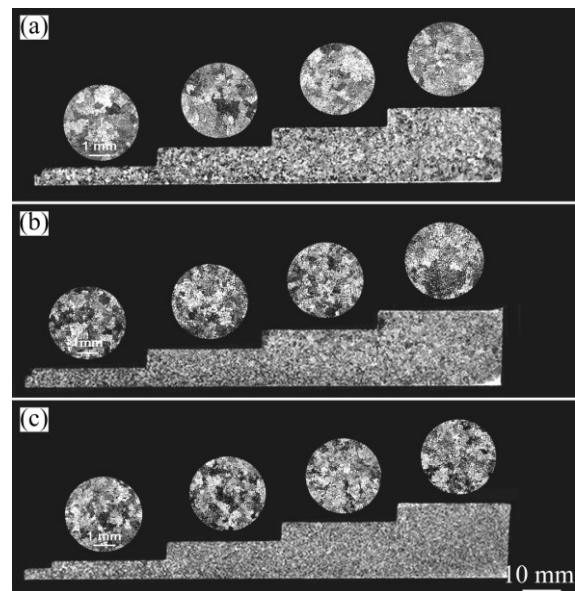


**Fig. 3** Grain structures of AlSi7Cu3Mg step castings: (a) Base alloy (Alloy 0); (b) Sr-modified alloy (Alloy 1); (c) Sr-modified and AlTi5B1 grain refined alloy (Alloy 2) [20]

step thickness from 5 to 20 mm (Figs. 3(a) and (b)). The macrographs reveal equiaxed grains throughout the castings and no columnar grains are present. Generally, this indicates that the heat extraction, which strongly depends on the casting geometry and process parameters, exceeds the rate of heat generated by the solidification process, independently of step thickness. As a result, the liquid undercools at a level that activates heterogeneous nuclei present in the liquid, producing multiple heterogeneous nucleation. Further, the undercooling decreases according to the thermal gradient in the castings, that is from thin to thick step.

The addition of AlTi5B1 grain refiner produces a uniform grain structure throughout the step castings. Fine and equiaxed grains are observed (Fig. 3(c)).

### 3.1.2 Cylinder head

Typical macrostructures of flame deck and bolt bosses drawn from cylinder heads after Sr modification and grain refinement are shown in Fig. 4.

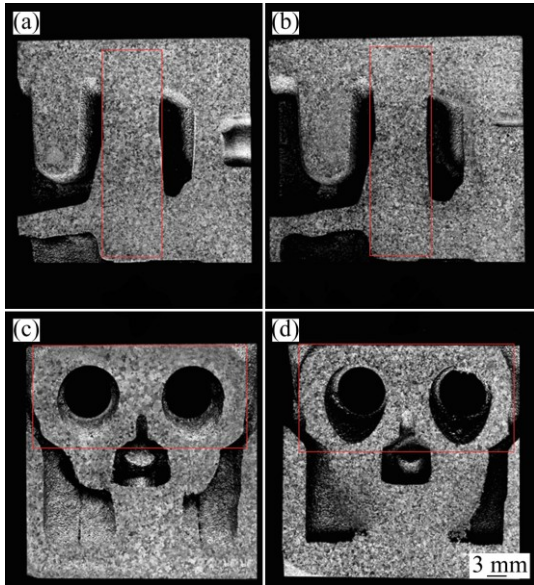


**Fig. 4** Grain structures of AlSi7Cu3Mg cylinder head in regions of bolt bosses (transversal section) (a, b) and flame deck (longitudinal section, ~4 mm under the casting surface) (c, d), indicated by red squares (The macrographs refer to Alloys 1 (a, c) and 2 (b, d), respectively)

In the Sr-modified alloy (Alloy 1), a non-homogenous grain structure is observed throughout the casting's sections (Figs. 4(a) and (c)). The macrographs reveal a complete equiaxed grain structure without columnar grains, independently of wall thickness. The flame deck (Fig. 4(c)) shows finer grains than bolt bosses (Fig. 4(a)). This is due to the position of the casting in the die, which enables higher solidification rate in the flame deck region. On the contrary, the application of sand cores, to obtain the complex geometry for cooling water-jacket inside the cylinder head, produces slower cooling rates with coarser grains. However, the cooling condition throughout the flame deck is not uniform as revealed by the grain structure. The highest values are localised around the valves, where the die receives a great amount of solidification heat from the casting. Further, the space between the valves (exhaust valves) of Fig. 4(c) is characterized by a non-homogeneous grain structure, i.e., fine and coarse grains coexist. This area is particularly critical because it reaches the highest temperatures on-service and is exposed to severe thermal fatigue effects when the engine warms up or cools down [28].

The AlTi5B1 grain refinement produces a uniform grain structure throughout the castings. Fine and

equiaxed grains are observed (Figs. 4(b) and (d)). This may be attributed to the increased number of TiB<sub>2</sub> and Al<sub>3</sub>Ti particles made available by grain refiner.

### 3.1.3 Quantitative comparison

Figure 5(a) shows the relation between the grain size and the step thickness as a function of the Sr modification and grain refinement. The high cooling rate in the 5 mm step produces a uniform and fine grain structure (~965 μm), independently of the modification or grain refiner level. By decreasing the cooling rate, the untreated or Sr-modified alloys (Alloy 0 and Alloy 1) present coarser grain size, that is ~1250 μm at 15 mm step thickness.

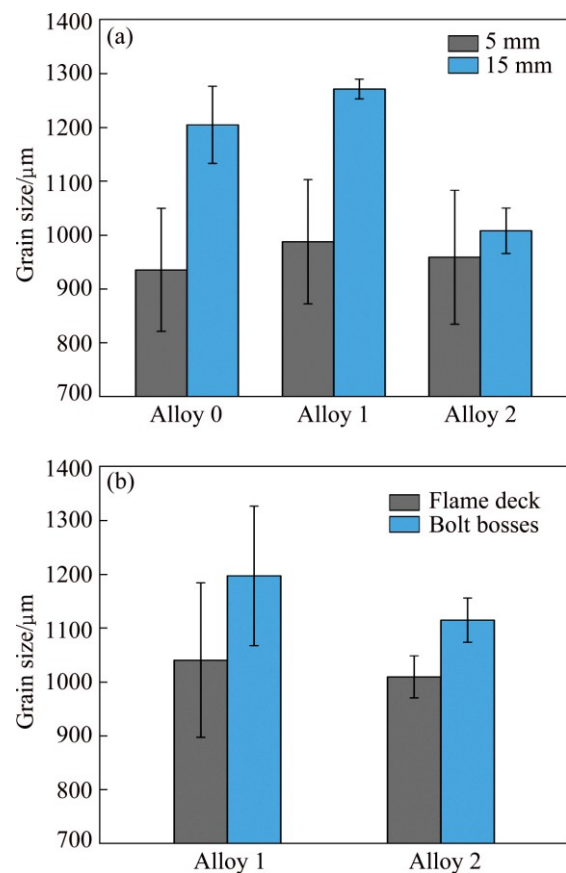


**Fig. 5** Variations of grain size for different step thickness (a) and regions of cylinder head (b) as function of experimental alloys

Considering the cylinder head (Fig. 5(b)), due to the high cooling rate, the flame deck shows an average grain size of ~1050 μm in the Sr-modified alloy (Alloy 1), while the macrostructural scale slightly decreases after the grain refinement (Alloy 2), with a reduction of the average grain size of ~3%. The greatest effect of grain refinement is observed on the dispersion of the grain size, as revealed by the standard deviations ( $\sigma$ ). A more uniform grain structure is obtained after AlTi5B1 addition with a standard deviation of ~40 μm, against 145 μm in the Sr-modified alloy.

The impact of grain refinement is more pronounced in the slowly solidified regions, i.e., bolt bosses, with ~7% reduction of the average grain size and a more uniform grain distribution with a standard deviation of 40  $\mu\text{m}$ .

The analysed steps present a grain size comparable with the macrostructural scale in the flame deck and bolt bosses of the cylinder head. Furthermore, the level of grain refinement achieved with the addition of AlTi5B1 is comparable in the two different casting geometries.

In commercial primary Al and Al alloys, it has been reported how the addition of Al–Ti–B master alloys guarantees the substrates for heterogeneous nucleation of primary  $\alpha(\text{Al})$  phase and increases the Ti content as solute in the liquid too. Titanium, segregating at the inoculant/melt interface, affects the growth of dendrites and leads to a constitutionally undercooled zone in front of the growing interface within which nucleation can occur on nucleants that are present [14]. It seems that in

Al–Si foundry alloys, the effects of both nucleants and segregated solute play an important role in an efficient refinement. In the present work, the supplied secondary AlSi7Cu3Mg alloy ingots contained an amount of 0.0411% Ti (mass fraction) as impurity, which was not sufficient to induce an effective growth-restriction of primary  $\alpha(\text{Al})$  and thus a complete grain refinement. The addition of AlTi5B1 grain refiner seems to be necessary to introduce stable nucleants, such as  $\text{TiB}_2$ , and the excess Ti solute is useful to reduce the grain growth of  $\alpha(\text{Al})$  crystals. Further, the presence of Sr does not produce any interaction or poisoning of AlTi5B1 grain refiner.

### 3.2 Microstructural observations

#### 3.2.1 Step casting

Typical microstructures of the step castings are shown in Fig. 6, referred to 5 and 15 mm steps and corresponding to the base AlSi7Cu3Mg alloy

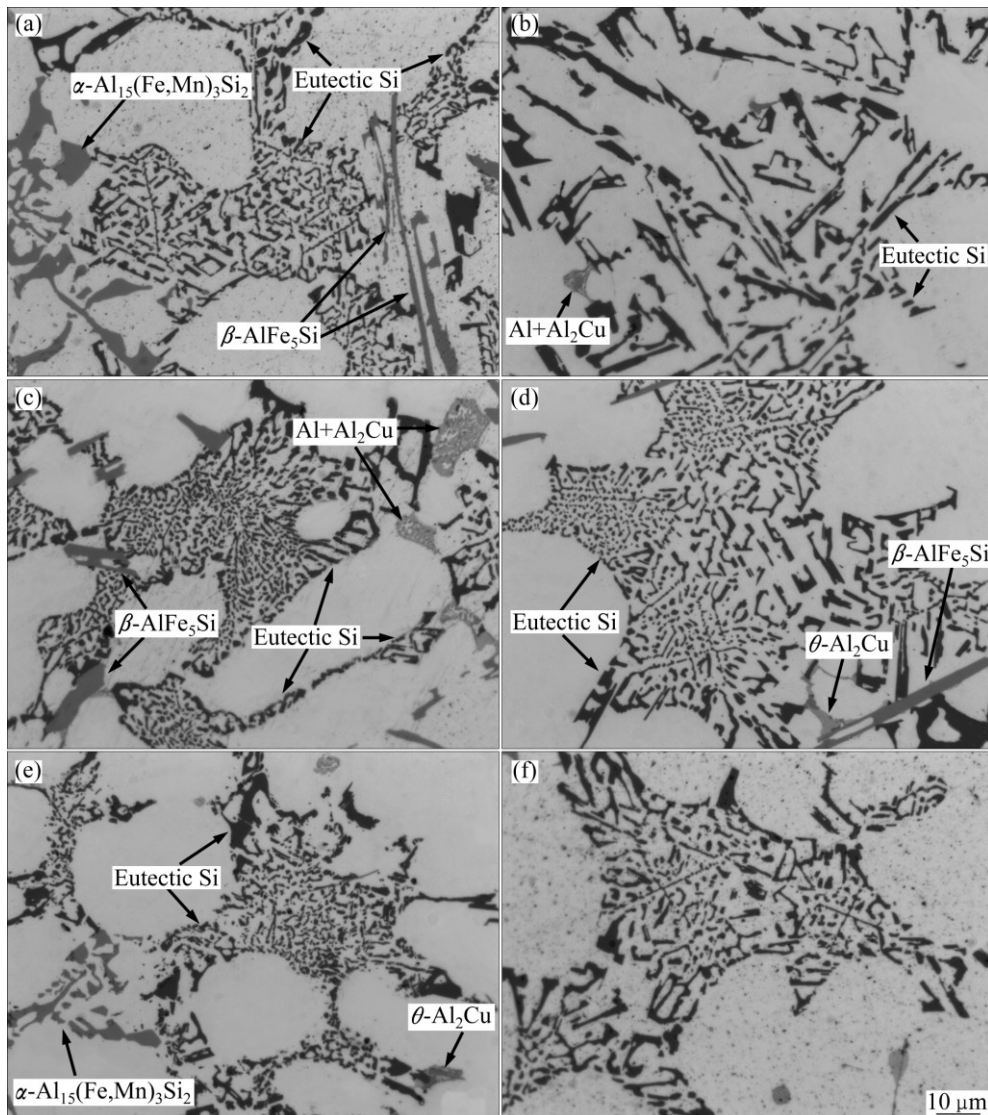


**Fig. 6** Eutectic silicon particles observed in 5 mm (a, c, e) and 15 mm (b, d, f) steps: (a, b) Base AlSi7Cu3Mg alloy (Alloy 0); (c, d) After Sr modification (Alloy 1); (e, f) after combined addition of Sr and AlTi5B1 (Alloy 2)

(Alloy 0), to the Sr-modified alloy (Alloy 1) and after Sr modification and AlTi5B1 grain refinement (Alloy 2), respectively.

The microstructure consists of a primary phase,  $\alpha(\text{Al})$  solid solution, and an eutectic mixture of Al and Si. The  $\alpha(\text{Al})$  precipitates from the liquid as the primary phase in the form of dendrites. Intermetallics compounds, such as Fe- and Cu-rich intermetallics, were also observed (see Fig. 6). The Fe-bearing particles are observed in the microstructure both in the form of coarse Chinese script  $\alpha\text{-Al}_{15}(\text{Fe,Mn})_3\text{Si}_2$  particles and needle-shaped  $\beta\text{-Al}_5\text{FeSi}$  phase. A high fraction of Cu-rich structures was detected in the form of both fine lamellae inside an  $\text{Al}+\text{Al}_2\text{Cu}$  eutectic structure in the interdendritic regions, and block-like  $\theta\text{-Al}_2\text{Cu}$  particles.

In the base alloy, the eutectic Si particles show a coarse plate-like morphology with coarser particles by increasing the step thickness (Figs. 6(a) and (b)). The highest cooling rate corresponding in the present work to the 5 mm step is not able to activate a quench modification [3].

The addition of nominal 0.01% Sr (mass fraction) produces a finer and fibrous eutectic Si, even in the 15 mm step (Figs. 6(c)–(f)). It is not difficult to conclude that the AlTi5B1 grain refiner has no poisoning effect on the Sr modification under the present casting conditions.

### 3.2.2 Cylinder head

Typical microstructures of the cylinder head are shown in Fig. 7, which refer to the flame deck and bolt

bosses, and correspond to the Sr-modified alloy (Alloy 1) and after the combined addition of Sr and AlTi5B1 (Alloy 2).

Due to Sr modification, the eutectic Si exhibits fine and fibrous morphology in both the analysed alloys and regions. Again, no evidence of any Sr poisoning mechanism by AlTi5B1 was found, reflecting the same results already obtained with the step castings.

### 3.2.3 Quantitative comparison

Generally, different casting thicknesses should produce different heat extraction rates and therefore different cooling rates. This is evident from the grain structure as well as the microstructural scale, which was here quantitatively estimated by means of SDAS measurements. The range of cooling rates was evaluated by SDAS that strictly depends on the cooling rate according to the empirical equation [29]:

$$\text{SDAS}=39.4R^{-0.317} \quad (3)$$

where  $R$  represents the mean cooling rate of the primary  $\alpha(\text{Al})$  dendrites during solidification. The SDAS values and the corresponding cooling rates are listed in Table 2.

The  $R$  values range between 0.9 and 5.5 °C/s, neither Sr nor AlTi5B1 affect it. On the other hand, the effects of Sr and AlTi5B1 on the eutectic Si morphology and the grain size are clear, but they had no impact on SDAS values which are still cooling rate dependant. The absence of any interaction between the AlTi5B1 grain refiner and the SDAS values is in accordance with the results from BIROL [30].

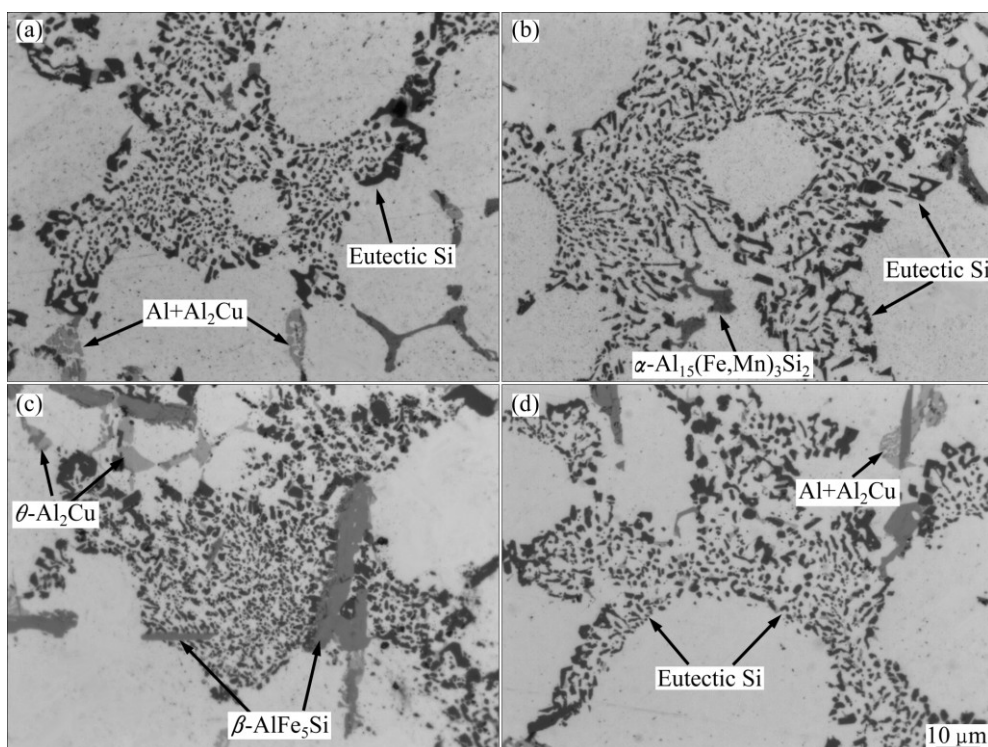


**Fig. 7** Typical microstructures of Sr-modified alloy (Alloy 1) (a, b) and after Sr modification and AlTi5B1 addition (Alloy 2) (c, d): (a, c) Regions of flame deck; (b, d) Bolt bosses

**Table 2** Average SDAS values measured in different steps and regions of cylinder head of experimental alloy

Location	Alloy No.	SDAS/ $\mu\text{m}$	Cooling rate/( $^{\circ}\text{C}\cdot\text{s}^{-1}$ )
Step 5 mm	0	$24 \pm 5$	4.8
	1	$24 \pm 7$	4.8
	2	$23 \pm 6$	5.5
Step 15 mm	0	$38 \pm 7$	1.1
	1	$41 \pm 10$	0.9
	2	$41 \pm 9$	0.9
Flame deck	1	$25 \pm 6$	4.2
	2	$26 \pm 6$	3.7
Bolt bosses	1	$42 \pm 10$	0.8
	2	$39 \pm 9$	1.0

Considering different heat extractions and cooling rates in the analysed regions, significant coarsening of the dendrite arms occurs during solidification of the bolt bosses and the 15 mm step, as revealed by great SDAS values,  $\sim 40 \mu\text{m}$  (Table 2); the flame deck and the 5 mm step show finer microstructure,  $\sim 25 \mu\text{m}$ . Furthermore, the 15 and 5 mm steps show SDAS values close to those obtained in the bolt bosses and flame deck, respectively.

On industrial casting production, it is difficult to obtain high solidification rate throughout the overall casting, therefore fine SDAS, for several reasons [31]: the complexity of the shape of cylinder heads, having many cavities in close proximity; the need for directional solidification to avoid casting macrodefects, and thus satisfactory quality in the final component; efficient heat removal is possible only close to the die walls; the gating and riser designs are influenced by the part geometry.

The eutectic Si particles shapes and sizes were quantitatively analysed and the main results are shown in Table 3.

The Sr effect on the aspect ratio of the eutectic Si particles is observed. The unmodified alloy (Alloy 0) shows mean values of aspect ratio of  $\sim 2.3$ , while in the Sr-modified alloys (Alloys 1 and 2), these values are reduced. For a defined alloy, no change of these features was observed in different analysed regions, i.e., no effect of cooling rate took place. On the contrary, the effect of cooling rate is evident on the dimension of the eutectic Si particles.

The AlTi5B1 grain refiner had no poisoning effect on the Sr modification under the present casting conditions. On the other hand, for the same location, no substantial change of the above discussed features was noted moving from Alloy 1 to Alloy 2.

**Table 3** Average values of size, roundness and aspect ratio of eutectic Si particles in different steps and regions of cylinder head as function of experimental alloy

Location	Alloy No.	Size/ $\mu\text{m}$	Aspect ratio
Step 5 mm	0	$1.2 \pm 1.2$	$2.1 \pm 0.9$
	1	$1.2 \pm 1.0$	$1.8 \pm 0.6$
	2	$1.2 \pm 1.1$	$1.7 \pm 0.5$
Step 15 mm	0	$1.7 \pm 1.4$	$2.4 \pm 1.1$
	1	$1.7 \pm 1.2$	$1.9 \pm 0.7$
	2	$1.4 \pm 1.2$	$1.9 \pm 0.7$
Flame deck	1	$1.1 \pm 1.2$	$1.9 \pm 0.7$
	2	$1.3 \pm 1.2$	$1.5 \pm 0.3$
Bolt bosses	1	$1.5 \pm 1.3$	$1.7 \pm 0.5$
	2	$1.5 \pm 1.1$	$1.7 \pm 0.5$

### 3.3 Mechanical testing

Several works [4,20,27,29,32–34] report how the mechanical properties of cast Al alloys are strongly affected by the secondary dendrite arm spacing. The general results evidence that the mechanical properties increase when SDAS decreases. The average tensile properties obtained in different regions of cylinder heads for the analysed alloys are listed in Table 4. Investigation results confirmed that increasing the cooling rate from the regions of bolt bosses to the flame deck improves the mechanical properties of as-cast AlSi7Cu3Mg alloy. For comparison, according to the EN 1706:2010 standard [35], the minimum mechanical properties of as-cast AlSi7Cu3Mg alloy, separately poured in a test-bar permanent mould, are 100 and 180 MPa for YS and UTS respectively, and 1% for elongation to fracture. In the present work, higher mechanical properties are due to both Sr modification and higher cooling rate respect to the separately cast test-bars.

**Table 4** Average mechanical properties obtained from different regions of cylinder head

Location	Alloy No.	YS/MPa	UTS/MPa	$s_{\sigma}/\%$	Quality index/MPa
Flame deck	1	$142 \pm 5$	$222 \pm 6$	$1.8 \pm 0.5$	$252 \pm 15$
	2	$154 \pm 9$	$224 \pm 4$	$2.2 \pm 0.2$	$274 \pm 17$
Bolt bosses	1	$130 \pm 5$	$200 \pm 4$	$1.6 \pm 0.1$	$231 \pm 15$
	2	$135 \pm 4$	$203 \pm 3$	$1.8 \pm 0.1$	$239 \pm 9$

The addition of AlTi5B1 grain refiner improves the mechanical behaviour of the Sr-modified cylinder heads, due to the change in the microstructure. The well-known Hall–Petch relationship shows that grain refinement is highly effective in improving the mechanical properties of materials. Fine equiaxed grain structure is desired

because it comes along with other several benefits such as uniform distribution of second phases and microporosity, improved feeding ability to avoid incomplete filling of mould, reduced porosity and the elimination of hot tearing and improved machinability of the products.

GRUZLESKI and CLOSSET [8] stated how the improvements carried out by grain refinement in Al–Si foundry alloys are mainly due to more uniform defects distribution rather than any decrease in grain size, and this leads to greater casting repeatability and reliability.

Several studies on cast metals has indicated how the Weibull distribution can reasonably describe the probability of fracture and the reliability of the casting process [26,27]. For Al castings, the two-parameter form of the Weibull distribution is widely adopted and can be expressed as

$$P_i = 1 - \exp[-(x/\eta)^\beta] \quad (4)$$

where  $P_i$  is the cumulative fraction of specimen failures (in tensile test) estimated according the Benard method [27];  $x$  is the variable being measured ( $Q$ );  $\eta$  is the scale parameter, i.e., the characteristic quality level at which 63.21% of the specimens has failed;  $\beta$  is the shape parameter, alternatively referred to as the Weibull modulus. The Weibull distribution can be converted into the linear form:

$$\ln\{\ln[1/(1-P_i)]\} = \beta \ln x - \beta \ln \eta \quad (5)$$

which can be easily plotted with  $\ln x$  and  $\ln\{\ln[1/(1-P_i)]\}$  as main axes. If the experimental distribution is Weibullian, a straight line will be produced with slope  $\beta$  and intercept  $-\beta \ln \eta$ . The slope  $\beta$  physically represents the Weibull modulus of the casting and it is clearly a measure of the spread of the distribution and repeatability of the castings.

Figure 8 shows the cumulative failure probabilities

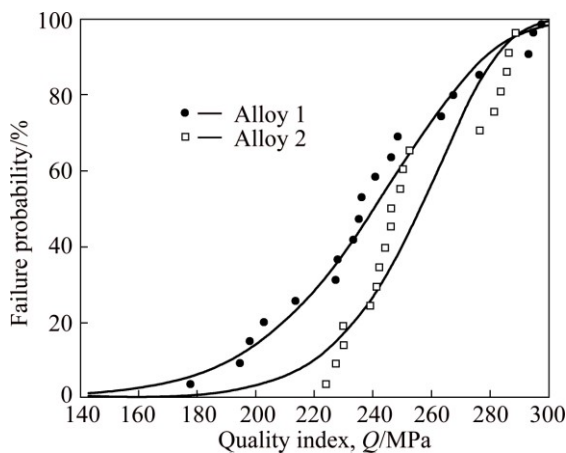


**Fig. 8** Cumulative failure probability for  $Q$  values of tensile specimens drawn from cylinder heads produced with different experimental alloys

of the tensile bars drawn from the cylinder heads produced with different alloys as a function of the quality index  $Q$ . The Weibull function, calculated according to Eq. (5), was used to fit the cumulative distributions. It is clear from the graph that the finest grain structure offered by the AlTi5B1 grain refiner (Alloy 2) strongly increases the reliability of the cast AlSi7Cu3Mg components.

It should be considered how the specimens drawn from the flame deck undergo higher cooling speed than the region of the bolt bosses, thus resulting in a finer microstructure. It seems logical, therefore, to exclude this bias to the Weibull results. The different analysed regions are distinguished in Fig. 9, where it is evident how the Weibull modulus is strongly affected by the regions of casting and grain refinement treatment. In general, higher  $\beta$  values are observed in the bolt bosses with respect to the flame deck. This behaviour can be attributed to the feeding mechanism in this region during the liquid–solid transaction as the bolt bosses are directly connected to the riser located at the top of the casting (see Fig. 4). The addition of AlTi5B1 (Alloy 2) produces a reduction of the average grain size and a more uniform grain distribution, especially in the region of the bolt

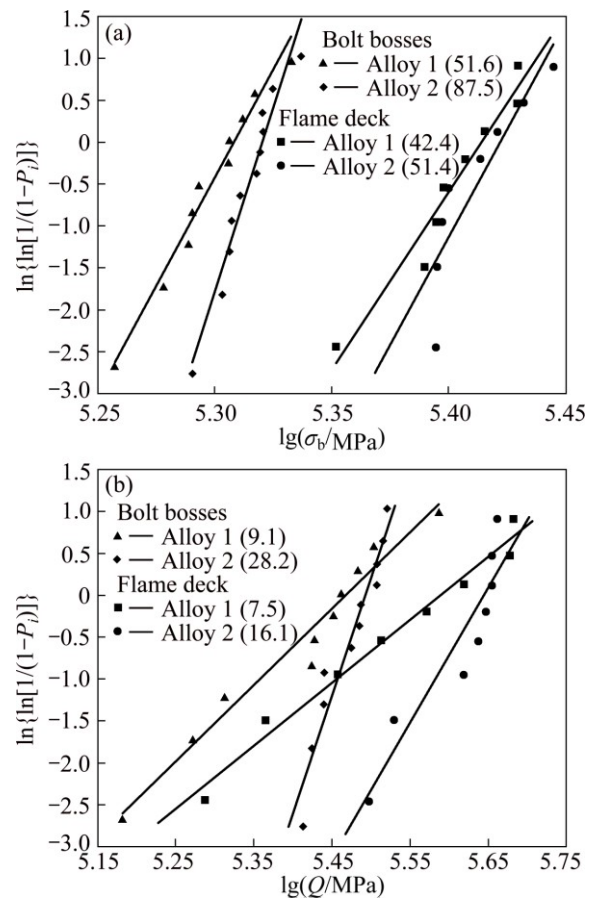


**Fig. 9** Weibull plots for UTS (a) and  $Q$  (b) values obtained from tensile test bars drawn from flame deck and bolt bosses of cylinder heads (The Weibull moduli of the analysed alloys are indicated in graph)

bosses (see Fig. 5). This leads to the increase of the coherency fraction solid and delay of the onset of dendrite coherency. It is therefore expected that the feeding process during solidification will continue for longer time with an overall reduction and distribution in porosity. Therefore, the addition of AlTi5B1 produces greater mechanical properties as shown in Table 4 and higher Weibull moduli, thus increasing throughout the reliability of the cylinder heads. For automotive structural components, such as cylinder heads, this could be considered as “an increase in safety” and useful to decrease the safety coefficients, i.e., wall thickness downsizing, which is important for both mass saving and reduction of the production cycle time.

## 4 Conclusions

1) The presence of Ti and B as impurity elements in the supplied secondary AlSi7Cu3Mg alloy is not sufficient to produce an effective grain refinement.

2) Decreasing the cooling rate, both the supplied and Sr-modified alloys exhibit a coarse and non-homogenous grain structure throughout the casting; on the contrary, the addition of AlTi5B1 grain refiner produces fine and uniform grains.

3) The improved effects of grain refinement are more pronounced in the slowly solidified regions of casting.

4) The combined addition of Sr and AlTi5B1 does not produce any reciprocal interaction or effect on primary  $\alpha(\text{Al})$  and eutectic solidification.

5) The tensile properties such as the yield strength, ultimate tensile strength, elongation to fracture and quality index increase by reducing the microstructural scale, i.e., increasing the cooling rate.

6) The grain refinement improves the mechanical properties of as-cast AlSi7Cu3Mg alloy.

7) The Weibull modulus  $\beta$  is strongly affected by the chemical grain refinement. The addition of AlTi5B1 produces higher Weibull moduli, thus increasing throughout the reliability of the casting. For automotive structural components, this could be considered as “an increase in safety”.

## References

- [1] ZEHNDER J, PRITZLAFF R, LUNDBERG S, GILMONT B. Aluminium in transport, aluminium in commercial vehicles [M]. 2nd ed., Brussels: European Aluminium Association, 2011: 7–13.
- [2] CROUSE W H, ANGLIN D L. Automotive engines [M]. 8th ed. New York: McGraw Hill, 1995: 71–75.
- [3] KHAN S, ELLIOTT R. Quench modification of aluminium–silicon eutectic alloys [J]. *Journal of Materials Science*, 1996, 31: 3731–3737.
- [4] GROSSELLE F, TIMELLI G, BONOLLO F. Doe applied to microstructural and mechanical properties of Al–Si–Cu–Mg casting alloys for automotive applications [J]. *Materials Science and Engineering A*, 2010, 527: 3536–3545.
- [5] GARCÍA-GARCÍA G, ESPINOZA-CUADRA J, MANCHA-MOLINAR H. Copper content and cooling rate effects over second phase particles behavior in industrial aluminium–silicon alloy 319 [J]. *Materials and Design*, 2007, 28: 428–433.
- [6] SCHLESINGER M E. Aluminum recycling [M]. Boca Raton: CRC Press, 2007: 176–192.
- [7] LIU Guang-lei, SI Nai-chao, SUN Shao-chun, WU Qin-fang. Effects of grain refining and modification on mechanical properties and microstructures of Al–7.5Si–4Cu cast alloy [J]. *Transactions of Nonferrous Metals Society of China*, 2014, 24(4): 946–953.
- [8] GRUZLESKI J E, CLOSSET B M. The treatment of liquid aluminium–silicon alloys [M]. Des Plaines: American Foundrymen’s Society, 1990.
- [9] MCCARTNEY D G. Grain refining of aluminium and its alloys using inoculants [J]. *International Materials Reviews*, 1989, 34: 247–260.
- [10] LIU Yuan, DING Chao, LI Yan-xiang. Grain refining mechanism of Al–3B master alloy on hypoeutectic Al–Si alloys [J]. *Transactions of Nonferrous Metals Society of China*, 2011, 21(7): 1435–1440.
- [11] EASTON M, STJOHN D H. Grain refinement of aluminum alloys: Part I. The nucleant and solute paradigms—A review of the literature [J]. *Metallurgical and Materials Transactions A*, 1999, 30: 1613–1623.
- [12] SCHUMACHER P, GREER A L, WORTH J, EVANS P V, KEARNS M A, FISHER P, GREEN A H. New studies of nucleation mechanism in aluminium alloys: Implications for grain refinement practice [J]. *Materials Science and Technology*, 1998, 14: 394–404.
- [13] SCHUMACHER P, MCKAY B J. TEM investigation of heterogeneous nucleation mechanisms in Al–Si alloys [J]. *Journal of Non-Crystalline Solids*, 2003, 317: 123–128.
- [14] CHANDRASHEKAR T, MURALIDHARA M K, KASHYAP K T, RAGHOTHAMA RAO P. Effect of growth restricting factor on grain refinement of aluminum alloys [J]. *International Journal of Advanced Manufacturing Technology*, 2009, 40: 234–241.
- [15] BINNEY M N, STJOHN D H, DAHLE A K, TAYLOR J A, BURHOP E C, COOPER P S. Grain refinement of secondary aluminium–silicon casting alloys [C]//*Proc TMS Light Metals*, 2003. San Diego, CA: TMS, 2003: 917–921.
- [16] ZHANG Y, MA N, YI H, LI S, WANG H. Effect of Fe on grain refinement of commercial purity aluminum [J]. *Materials and Design*, 2006, 27: 794–798.
- [17] SPITTLE J A, SADLI S. Effect of alloy variables on grain refinement of binary aluminium alloys with Al–Ti–B [J]. *Materials Science and Technology*, 1995, 11: 533–537.
- [18] BUNN A M, SCHUMACHER P, KEARNS M A, BOOTHROYD C B, GREER A L. Grain refinement by Al–Ti–B alloys in aluminium melts: A study of the mechanisms of poisoning by zirconium [J]. *Materials Science and Technology*, 1999, 15: 1115–1123.
- [19] TIMELLI G, CAPUZZI S, BONOLLO F. Optimization of a permanent step mold design for Mg alloy castings [J]. *Metallurgical and Materials Transactions B*, 2015, 46: 473–484.
- [20] TIMELLI G, CAMICIA G, FERRARO S. Effect of grain refinement and cooling rate on the microstructure and mechanical properties of secondary Al–Si–Cu alloys [J]. *Journal of Materials Engineering and Performance*, 2014, 23: 611–621.
- [21] VANDER VOORT G F. Metallography: Principles and practice [M]. New York: McGraw-Hill, 1984: 612.
- [22] ASTM E112-12. Standard test methods for determining average grain size [S].
- [23] ISO 6892-1. Metallic materials—Tensile testing—Part 1: Method of test at room temperature [S].
- [24] DROUZY M, JACOB S, RICHARD M. Interpretation of tensile results by means of quality index and probable yield strength [J].

- International Cast Metals Journal, 1980, 5: 43–50.
- [25] ALEXOPOULOS N D. Definition of quality in cast aluminum alloys and its characterization with appropriate indices [J]. Journal of Materials Engineering and Performance, 2006, 15: 59–66.
- [26] TENG X, MAE H, BAI Y. Probability characterization of tensile strength of an aluminum casting [J]. Materials Science and Engineering A, 2010, 527: 4169–4176.
- [27] GREEN N R, CAMPBELL J. Statistical distributions of fracture strengths of cast Al–7Si–Mg alloy [J]. Materials Science and Engineering A, 1993, 173: 261–266.
- [28] NICOLETTO G, RIVA E. Elevated temperature fatigue behavior of cast aluminum alloys used for I.C. engine part production [J]. Metallurgia Italiana, 2011, 103: 41–48.
- [29] WANG Q G, CÁCERES C H. Mg effects on the eutectic structure and tensile properties of Al–Si–Mg alloys [J]. Material Science Forum, 1997, 242: 159–164.
- [30] BIROL Y. Impact of grain size on mechanical properties of AlSi7Mg0.3 alloy [J]. Materials Science and Engineering A, 2013, 559: 394–400.
- [31] ZHANG B, GARRO M, TAGLIANO C. Dendrite arm spacing in aluminium alloy cylinder heads produced by gravity semi-permanent mold [J]. Metallurgical Science and Technology, 2003, 21: 3–9.
- [32] DOBRZANSKI L A, MANIARA R, SOKOŁOWSKI J H, KASPRZAK W. Effect of cooling rate on the solidification behavior of AC AlSi7Cu2 alloy [J]. Journal of Materials Processing Technology, 2007, 191: 317–320.
- [33] DOBRZANSKI L A, MANIARA R, SOKOŁOWSKI J H. The effect of cooling rate on microstructure and mechanical properties of AC AlSi9Cu alloy [J]. Archives of Materials Science and Engineering, 2007, 28: 105–112.
- [34] GROSSELLE F, TIMELLI G, BONOLLO F, TIZIANI A, DELLA CORTE E. Correlation between microstructure and mechanical properties of Al–Si cast alloys [J]. Metallurgia Italiana, 2009, 101: 25–32.
- [35] EN 1706. Aluminium and aluminium alloys—Castings—Chemical composition and mechanical properties [S].

## 重力铸造汽车气缸盖用 AlSi7Cu3Mg 二次合金的晶粒细化

Giordano CAMICIA, Giulio TIMELLI

Department of Management and Engineering,

University of Padova, Stradella S. Nicola, 3 I-36100 Vicenza, Italy

**摘要:** 研究了 AlTi5B1 晶粒细化和冷却速率对 AlSi7Cu3Mg 二次合金显微组织和力学性能的影响。采用阶梯铸模在不同冷却速率下制备添加晶粒细化剂的合金，并利用金相和图像分析技术定量研究了合金的宏观组织和显微组织。研究表明，添加 AlTi5B1 后，整个铸件具有细小均匀的晶粒组织，且在慢速凝固区域效果更显著。当冷却速率增加时，少量细化剂就可使铸件获得细小均匀组织。另外，原材料中的 Ti 和 B 以杂质的形式存在，不足以形成有效的晶粒细化效果。利用阶梯铸造法的研究结果研究了重力半固模铸造 16V 汽油发动机气缸盖。Weibull 统计结果表明，晶粒细化改善了合金的塑形变形行为，提高了铸件的可靠性。

**关键词:** 铝合金；晶粒细化；阶梯铸造；气缸盖；冷却速率；显微组织；力学性能

(Edited by Yun-bin HE)